

## ON THE SEISMIC WAVES REFLECTED AT THE MOHOROVIĆ DISCONTINUITY (II)

BY

Akira KAMITSUKI

(Received March 20, 1958)

### 1. Introduction

Recently the investigation of the earth's crust has developed remarkably. Above all, the method using seismic waves which are transmitted through the crust is considered to be the most direct and powerful. Up to the present time, it was ascertained that the earth's crust usually consists of several layers separated by discontinuity surfaces. It was found that the crustal structure has the significant contrast between continents and ocean basins and has local difference from place to place. Furthermore, in America and some other regions, it is suggested that there may be a low-velocity layer in which the velocities of seismic waves decrease with the increase of depth. Thus more detailed discussions on the earth's crust need to be carried out.

In general, the records of near earthquakes are the major sources of information about the earth's crust, but practically speaking, various effects are superposed on one another, and the records are greatly complicated. Then it must be considered that these effects should be selected separately by some instrumental device and be caught with much certainty. On the other hand, it is also desirable for the observation stations to be distributed as densely as possible so that many records are available in the proper range of distance. And not only the travel time, but also the amplitude, period, wave form and other elements of seismograms should be traced continuously with distance and azimuth. From these more detailed informations about the earth's crust will be able to be obtained.

In seismometric analysis, there are different sorts of method of using the refraction, reflection, dispersion of surface waves and others. In the analysis of near earthquakes, the refracted waves are mainly investigated, that is,  $P^k$  and  $P_n$  of  $P$ -group or corresponding  $S^*$  and  $S_n$  of  $S$ -group, but movements between  $P$ - and  $S$ -phases are less studied. Jeffreys and Bullen suggested that these movements may be caused by the strong repeated reflection of bodily waves between the earth's outer surface and the crustal discontinuity (1, 2). These phases were interpreted as  $pP$ ,  $PP$ , etc. in analogy to distant earthquake by some researchers (3), but in this interpretation there is a disagreement in travel time relation. And there remain still

insolvable characters (4, 5, 6). Furthermore, in the part after *S*, the strong phases are frequently recognized but in this case, the appearance of surface waves should be considered together (7, 8, 9).

In our previous paper (Part I), the seismograms of near earthquake within about 100 km were studied, taking special account of the primary reflection of *S*-wave at some crustal discontinuities. As a continuation of Part I, the seismograms of shallow-seated earthquake recorded in the distance range from about 100 km to 600 km are investigated in the present paper, and the parts of seismograms between the *P*- and *S*-waves are mainly studied and its relations to the earth's crust are discussed in some detail.

## 2. The earthquakes of March 7, 1952 and July 27, 1955

Considering the conditions to have shallow-seated origin in the crust and to be observed at as many stations as possible, the following two earthquakes were selected.

Earthquake	(1) The Daishoji-OkI	(2) The Tokushima
Origin time	1952, March, 7 <sup>d</sup> 16 <sup>h</sup> 32 <sup>m</sup>	1955, July, 27 <sup>d</sup> 10 <sup>h</sup> 20 <sup>m</sup>
Epicenter	36°28'N, 136°12'E	33°45'N, 134°18'E
Focal depth	20 km	0~10 km
Greatest distance of human feeling	770 km	670 km

The former caused comparatively little damage on land owing to its epicenter located off sea coast and 152 aftershocks were registered in March (10), while slight damage was caused by the latter at the epicentral region in Tokushima Prefecture (11). In order to develop the following investigation, the original seismograms recorded at the Abuyama and Kamigamo Observatories and the copied seismograms recorded at the Japan Meteorological Observatories were available. The total number of stations concerned is 32 in all. In the case of the Daishoji-OkI Earthquake, the data used were from 25 stations extending from 130 km to 670 km, and in the case of the Tokushima Earthquake, those from 24 stations extending from 40 km to 540 km were used. The locations of epicenters and stations are shown in Fig. 1.

In the following, the parts of the seismograms from the initial *P*-motion to the principal *S*-motion are studied, analysing the travel time, amplitude, period and wave form of each phase.

### a) *Travel time-distance graph*

In the first place, the arrival times of three phases in the forerunning part of *P*-wave and of the corresponding ones of *S*-wave are measured. The observed values are tabulated in Tables I and II.

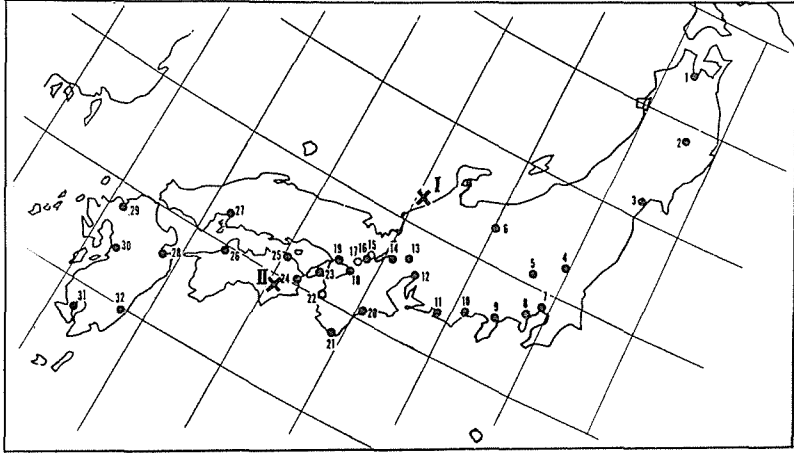


Fig. 1. The locations of epicenters and stations tabulated in Tables I and II.

Epicenters :—

(I) The Daishoji-Oki Earthquake

(II) Tokushima Earthquake

Stations :—

- |                              |                                   |                               |               |
|------------------------------|-----------------------------------|-------------------------------|---------------|
| 1. Aomori                    | 2. Morioka                        | 3. Sendai                     | 4. Utsunomiya |
| 5. Kumagaya                  | 6. Nagano                         | 7. Tokyo                      | 8. Yokohama   |
| 9. Mishima                   | 10. Shizuoka                      | 11. Hamamatsu                 | 12. Nagoya    |
| 13. Gifu                     | 14. Hikone                        | 15. Kamigamo<br>(Kyoto Univ.) | 16. Kyoto     |
| 17. Abuyama<br>(Kyoto Univ.) | 18. Osaka                         | 19. Kobe                      | 20. Owashi    |
| 21. Shionomisaki             | 22. Yuasa<br>(Taikyū High School) | 23. Sumoto                    | 24. Tokushima |
| 25. Takamatsu                | 26. Matsuyama                     | 27. Hiroshima                 | 28. Oita      |
| 29. Fukuoka                  | 30. Kumamoto                      | 31. Kagoshima                 | 32. Miyazaki  |

To calculate the epicentral distance, the epicenters reported in the Seismological Bulletin published by the Japan Meteorological Agency are accepted and the following formula is used :

$$2(1 - \cos \Delta) = (A - A')^2 + (B - B')^2 + (C - C')^2,$$

where  $\Delta$  is the epicentral distance in degree and  $A, B$  and  $C$  of epicenter are defined by

$$A = \cos \theta \cos \phi, \quad B = \cos \theta \sin \phi, \quad C = \sin \theta.$$

Here,  $\theta$  is the geocentric latitude,  $\phi$  is the east longitude, and  $A', B', C'$  are the corresponding parameters for each station. The travel time-distance graphs of these two earthquakes are shown in Figs. 2 and 3 respectively. In these figures, the travel times before and after the direct  $P$ -wave ( $\bar{P}$ ) are taken against the epicentral distance. (Especially, the travel times of initial motion reported in the Seismological Bulletin are also plotted in Figs. 2 and 3. Then the total number of stations is 59 in the former and 54 in the latter.)

Table I. Arrival time of each phase of the Daishoji-Oki Earthquake.  
Station numbers are shown in Fig. 1.

No.	Station	$d$	Arrival time										
			$P_n$	$P^*$	$\bar{P}$	$R_1$	$R_2$	$R_3$	$R_4$	$S_n$	$S^*$	$\bar{S}$	
		km	m s	m s	m s	m s	m s	m s	m s	m s	m s	m s	m s
13	Gifu	133			33 1.9								
14	Hikone	133			1.4								
12	Nagoya	161	33 4.2										34 23.1
16	Kyoto	167	6.0			33 17.5							26.9
6	Nagano	180											
18	Osaka	211			15.5		33 31.5						41.3
19	Kobe	219	12.9		17.0	20.3	31.9	33 37.4				33 40.2	44.7
10	Shizuoka	260	18.9		23.7	30.4	35.2	43.1				51.4	
23	Sumoto	265	19.0		23.7	30.3	36.7	41.6				47.6	55.9
5	Kumagaya	289	23.8		30.5	33.4	40.9	50.0				56.5	34 3.2
9	Mishima	289	23.0		29.9	33.2	39.7	49.7				55.7	2.8
24	Tokushima	306	25.0	33 27.9	31.8	36.2	42.5	52.5				34 3.0	7.6
25	Takamatsu	310	25.0	27.1	31.2	38.5	45.0	51.0			33 58.8		8.0
4	Utsunomiya	328	27.8		37.1	39.2	46.3	56.3				8.5	16.9
8	Yokohama	332	27.6	32.2	37.5	39.3	49.6	55.0			34 3.2	9.6	15.8
7	Tokyo	332	27.6		37.5		49.1	54.4				8.3	19.7
27	Hiroshima	419	38.7	42.3	49.0	54.7	34 2.1	34 9.7	34 18.8		22.6	29.7	40.7
26	Matsuyama	426	38.8										44.2
3	Sendai	461	45.4	50.1	55.5		7.3	14.0	22.6	30.7	41.0	53.8	
28	Oita	552	55.9	34 2.8	34 9.8		21.1	29.3	37.5	50.5	58.6	35 15.1	
2	Morioka	565	57.4										
29	Fukuoka	621	34 5.9		22.7		29.8	40.2	48.0			35 21.7	38.0
1	Aomori	625	5.8										
30	Kumamoto	647	5.2	14.6	25.3		33.7	41.4	48.2	35 9.8	21.7	46.4	
32	Miyazaki	669	10.6		32.2			45.8	55.6				53.5

Table II. Arrival time of each phase of the Tokushima Earthquake.  
Station numbers are shown in Fig. 1.

No.	Station	<i>d</i>	Arrival time												
			<i>P<sub>n</sub></i>	<i>P*</i>	$\bar{P}$	<i>R<sub>1</sub></i>	<i>R<sub>2</sub></i>	<i>R<sub>3</sub></i>	<i>R<sub>4</sub></i>	<i>R<sub>5</sub></i>	<i>R<sub>6</sub></i>	<i>S<sub>n</sub></i>	<i>S*</i>	$\bar{S}$	
24	Tokushima	46 km	m s	m s	m s	m s	m s	m s	m s	m s	m s	m s	m s	m s	m s
					20 58.5										21 3.6
25	Takamatsu	67			21 2.3										11.8
22	Yuasa	87			6.3										18.5
23	Sumoto	87			4.0										
21	Shionomisaki	141		21 15.0	16.2	21 19.5	21 23.9								32.1
26	Matsuyama	141		14.6	16.4	18.7	24.3	21 28.7							31.9
17	Abuyama	171	21 19.0		21.8	24.7									41.3
20	Owashi	180	19.0		23.2		33.4						21 40.1		44.4
27	Hiroshima	185	21.3		23.7	27.0	33.3	39.9					43.0		45.2
15	Kamigamo	198	22.4		26.7	29.8	33.5	40.9				21 44.8			48.2
14	Hikone	247	29.1		34.8	37.1	41.5	45.9	21 52.1			56.8		21 2.3	
28	Oita	256		32.8	36.7		41.9	45.7	52.0				59.8	9.7	
12	Nagoya	291	34.5		41.2			49.2	55.7	22 0.6			22 10.8	16.8	
13	Gifu	291	34.9		42.8		45.1	51.9	57.9	3.3			10.7	17.9	
32	Miyazaki	326	40.3	43.3	50.6			55.5	22 2.2		22 5.1		16.5	29.4	
11	Hamamatsu	332	40.9		49.5				2.5				26.3	31.8	
30	Kumamoto	350	40.9	47.5	53.6			58.7	5.3	12.0	16.7	22 20.3	28.5	35.8	
29	Fukuoka	363	43.0		52.6			57.9	4.8	10.1				38.3	
10	Shizuoka	400	47.8		22 0.8			22 7.8	16.2	20.5		28.6	33.8	48.3	
31	Kagoshima	426	50.5	55.4	4.8			10.8	18.9	23.2	31.1	34.9	42.3	56.6	
9	Mishima	452	53.8	59.5	10.6			16.9	21.8		33.5	40.3	52.5	23 6.1	
8	Yokohama	524	22 2.6												
5	Kumagaya	536	6.4	22 12.1	20.6				31.4	36.8	46.7	23 1.0	23 17.6	28.4	
7	Tokyo	545	8.3		21.5			27.7	32.9				16.5	31.9	

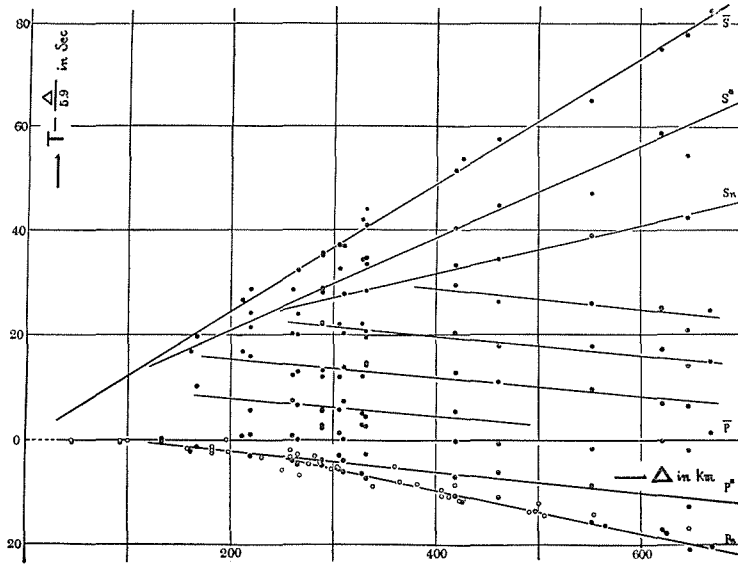


Fig. 2. Travel time-distance graph of the Daishoji-Oki Earthquake tabulated in Table I.

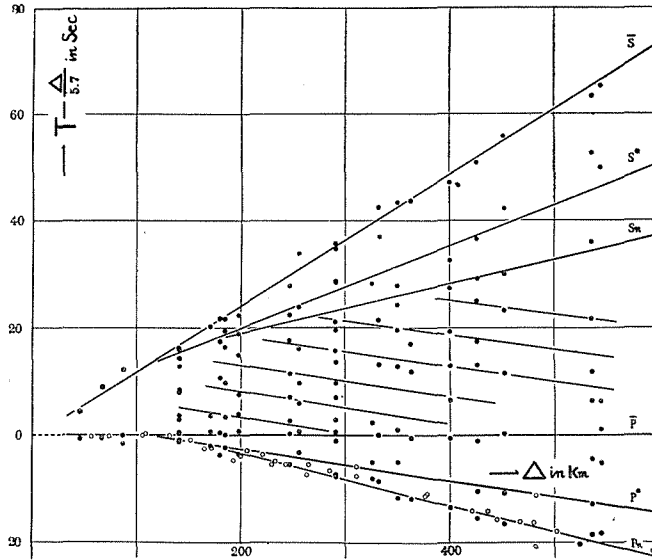


Fig. 3. Travel time-distance graph of the Tokushima Earthquake tabulated in Table II.

In the previous investigations it was stated that in our country, the crustal structure has a local difference and its thickness varies from place to place in the range between 25 km and 50 km. And moreover, its diversity is mainly due to the lowest layer, i.e. the basaltic layer (12, 13, 14). Relating to this fact, in the present analysis, the forerunning parts of the two earthquakes have a significant difference. Usually in the distance beyond about 100 km, the  $P^*$ -wave and the  $P_n$ -wave succeeding it appear before the arrival of direct  $P$ -wave. In the case of the Daishoji-Oki Earthquake, the distance range in which the  $P^*$ -wave is the first motion, is wider than in the case of the Tokushima Earthquake. And in the latter, the identification of the  $P^*$ -wave as the second phase in larger distances is rather difficult. This corresponds to the fact that the basaltic layer is thicker in the mountain area of the central part of Honshu than in the district of Shikoku and Kii Peninsula. In the next, the phases of  $S$ -group are less identifiable than the corresponding ones of  $P$ -group, especially in the cases of  $S^*$  and  $S_n$ . By the method of least squares, the velocities of each phase are calculated as follows.

	The Daishoji-Oki Earthquake	The Tokushima Earthquake
$\bar{P}$	5.9 km/sec	5.7 km/sec
$P^*$	6.9	7.0
$P_n$	8.0	7.9
$\bar{S}$	3.4	3.3
$S^*$	4.0	4.0
$S_n$	4.7	4.6

After these preliminary investigations the parts of the seismograms between  $P$ - and  $S$ -waves are studied in detail. In such part, the displacement traced at any observation station is usually much complicated in appearance. It is found, however, that the several pulses recur successively in about equal time interval. The arrival times of these successive phases are tabulated in Tables I and II, and are plotted against the epicentral distance in Figs. 2 and 3. The typical examples of such records are shown in Figs. 4, 5, 6, 7, 8, 9 and 10. These are recorded at stations of epicentral distances of 265 km, 419 km, 552 km and 647 km in the case of the Daishoji-Oki Earthquake, and 256 km, 291 km and 536 km in the case of the Tokushima Earthquake respectively. Connecting these phases from station to station continuously, the curves of  $R_1$ ,  $R_2$ ,  $R_3$ , etc. are drawn. Then, (1) their apparent velocities have the values between those of the  $\bar{P}$  and  $P_n$  and (2) they appear successively in about equal time interval after the direct  $P$ -wave. From these facts, they should be interpreted to be the multiple reflections of  $P$ -wave between the earth's outer surface and the Mohorovičić discontinuity. Moreover, the time intervals between them are about from 7 sec to

10 sec in the Daishoji-Oki Earthquake and from 5 sec to 7 sec in the Tokushima Earthquake. These values show their clear dependence on the crustal thickness of each region through which the multiple reflected waves are transmitted. The former value corresponds to the thickness of about 40 km and the latter to the 30 km, respectively.

In general the seismic wave impinging upon the discontinuity surface generates the reflected and refracted waves and suffers the change of type from  $P$  to  $S$  or *vice versa*. Then, in the records of near earthquake, there can be a large number of phases theoretically. But the change of type at the interface involving the Mohorovičić discontinuity usually causes considerable diminishing of amplitudes except the case at the free surface (1, 15, 16, 17). Therefore the composite waves which suffer the change of type at the internal discontinuity encountered may be left out of consideration. The multiple reflections between the outer free surface and the  $g$ - $b$  discontinuity (between granitic layer and basaltic layer) have no need to be considered, because they arrive much earlier and have smaller amplitude than the phases discussed in the present study. But it may not be distinguishable in the point of arrival time and amplitude, whether the wave starts initially upward to the outer free surface or downward to the base reflector. Taking account of these conditions, the number of phases to be observable is fairly reducible. In order to verify the above-mentioned identification from the travel time, the amplitude investigation should be made in addition.

#### b) *Amplitude- and period-relation*

As mentioned earlier, in the records of near earthquakes many phases may be identifiable. But there is frequently much ambiguity in their identifications owing to the scattering or clustering of plotted points in the travel time-distance graph. In order to avoid such arbitrariness, it is desirable that the data of as many stations as possible be available and besides, the changes of amplitude, period, wave form, etc. with epicentral distance which may characterize these phases, be investigated concurrently. Then they can be connected continuously from station to station and their reliability will be increased. For this purpose, it was favourable that the seismographs equipped at the stations concerned in the present study are all of the same type except a few (Tokushima, Hamamatsu and Matsuyama), that is, the small Wiechert seismograph which has the following constants.

Component	Weight of mass	Magnification	Period	Damping ratio
Horizontal	200 kg	60~100	4~5 sec	5~7
Vertical	80 kg	50~ 80	4~5 sec	5~7



In the following study of amplitude, the vertical component is mainly studied, because it contains theoretically the waves of  $P$ - and  $SV$ -types only. On the other hand, in the horizontal component the polarization and azimuth of station as seen from the epicenter must be considered in addition. Observed values are tabulated in Tables III and IV.

Table III. Observed amplitude of each phase (vertical component) of the Daishoji-Okii Earthquake. Station numbers are shown in Fig. 1.

No.	Station	$\Delta$	Amplitude						
			$P_n$	$\bar{P}$	$R_1$	$R_2$	$R_3$	$R_4$	$\bar{S}$
		km	$\mu$	$\mu$	$\mu$	$\mu$	$\mu$	$\mu$	$\mu$
	Kanazawa	45		700					
14	Hikone	133		449					
12	Nagoya	161	135	405					—
6	Nagano	180	62	402					
	Kameyama	182		457					
18	Osaka	211		336					
19	Kobe	219	110	193	131	56	65		280
	Kofu	230	33						
10	Shizuoka	260	69	136	118	80	89		—
23	Sumoto	265	30	125	198	75	63		262
20	Owashi	267	23						
9	Mishima	289	29	122	108	70	110		396
5	Kumagaya	289	28	142	94	175	163		181
4	Utsunomiya	328	10	100	72	123	123		460
8	Yokohama	332	22	110					
7	Tokyo	332	50	156	81	148	173		425
27	Hiroshima	419	15	103	35	21	40	28	256
26	Matsuyama	426	16						
28	Oita	552	17	91		91	56	60	212
29	Fukuoka	621	10	55		30	25	25	225
30	Kumamoto	647	15	42		26	38	26	122

In Figs. 11 and 12, the amplitude of each phase is plotted against the epicentral distance. The points are rather scattered. This may be due to the emission mechanism at the origin, the locality of each station, the instrumental effect, etc. Then, especially the amplitudes of  $\bar{P}$  and  $P_n$  are taken up and they are adjusted to the mean curves respectively, and the other phases are plotted according to such adjustment.

On the other hand, the theoretical calculation is made under the following assumptions and the result is shown in Fig. 13.

- 1) The crustal structure as shown in the previous paper (I) is used and the origin is situated at depth of 20 km (14).

- 2) At the origin, the equal energy is emitted in all directions.
- 3) The reflection and refraction coefficients of waves at each discontinuity are calculated as for plane waves (16, 18, 19, 20, 21, 22).
- 4) Divergence effect of spreading of waves and absorption effect due to the crustal structure are neglected.

The dominant factors in the calculation are the reflection coefficients at both the free surface and the Mohorovičić discontinuity as the upper and lower boundaries. And the refractions at the interfaces elsewhere have scarcely any influence upon the calculated values.

Comparing the observed and calculated curves, we see that they are generally in good accordance with each other. It is found that as the number of multiple increases, the amplitude curves of respective phases have its own peak successively

Table IV. Observed amplitude of each phase (vertical component) of the Tokushima Earthquake. Station numbers are shown in Fig. 1.

No.	Station	$\Delta$	Amplitude								
			$P_n$	$\bar{P}$	$R_1$	$R_2$	$R_3$	$R_4$	$R_5$	$R_6$	$\bar{S}$
		km	$\mu$	$\mu$	$\mu$	$\mu$	$\mu$	$\mu$	$\mu$	$\mu$	$\mu$
	Muroto	57		700							
25	Takamatsu	67		460							645
	Kochi	74		328							
23	Sumoto	87	109	—							—
21	Shionomisaki	141	107	175	315	64					452
26	Matsuyama	141	100	173	168	171	75				268
17	Abuyama	171	40	140							410
20	Owashi	180	44	152		57					272
27	Hiroshima	185	33	172	120	100	71				380
15	Kamigamo	198	15	140	100	144					331
	Toyooka	200	28								
	Kameyama	234	38								
	Hamada	243	3								
14	Hikone	247	20	67		53	87				430
28	Oita	256	20	123		90	94	185			400
12	Nagoya	291	20	73			52	20	47		434
13	Gifu	291	—	50		60	28	50	68		280
32	Miyazaki	326	3	17							110
30	Kumamoto	350	4	55			26	22		22	129
29	Fukuoka	363	12	50							
10	Shizuoka	400	9	27			23		21		192
31	Kagoshima	426	2	12			35	27		42	92
9	Mishima	452	6	36			21	17		25	64
5	Kumagaya	536	5	17				18	17	15	285

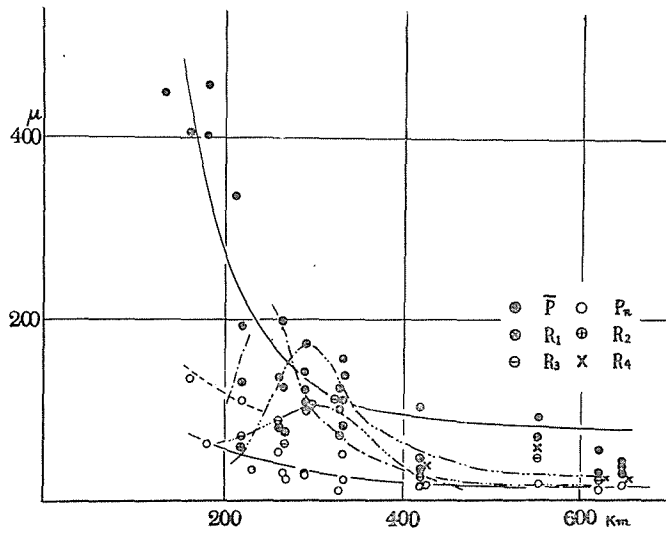


Fig. 11. Observed amplitude-distance graph (vertical component) of the Daishoji-Oki Earthquake.

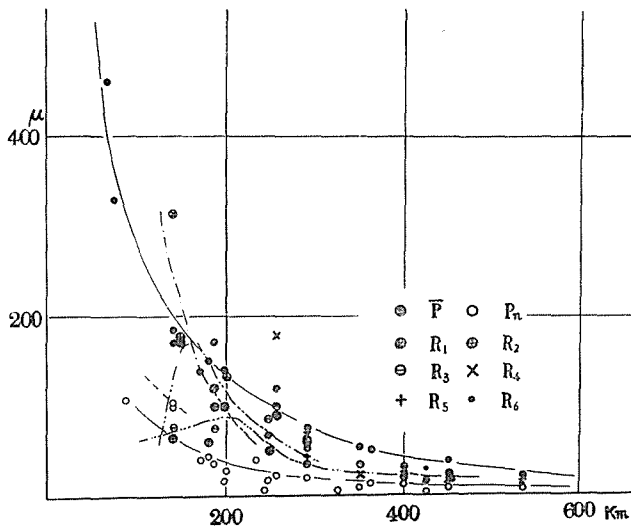


Fig. 12. Observed amplitude-distance graph (vertical component) of the Tokushima Earthquake.

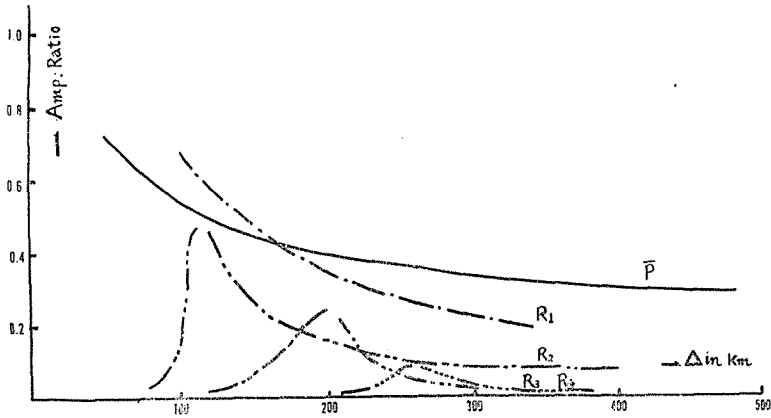


Fig. 13 Theoretical amplitude-distance graph (vertical component).

in the particular distance and their maximum value sometimes exceeds the value of direct  $P$ -wave. In the case of the Daishoji-Oki Earthquake, this is clearly shown in Fig. 4 recorded at Sumoto ( $\Delta=265$  km). At that distance, the large phase of  $R_1$  follows the direct  $P$ -wave.

In the case of the Daishoji-Oki Earthquake, the later phases,  $R_3$  and  $R_4$ , and in the case of the Tokushima Earthquake,  $R_3$ ,  $R_4$ ,  $R_5$  and  $R_6$  prevail over a wider range of distance, and moreover, their periods are longer than those earlier all over the range concerned as shown in Figs. 11 and 12. Their periods are likely those of the  $S$ -group.

Continuing to trace the amplitude variation beyond about 500 km, the periods of the direct  $P$ -wave and the successive phases in the following part become longer and longer one after another forming a wave train in a beat-like form, as shown in Figs. 7 and 10. Relating to these points, Gutenberg suggested that the direct  $P$ -wave at distances greater than about 100 km is the channel wave through the low-velocity layer (23). Further study about these points will be necessary.

### 3. Some considerations

In the seismic prospecting, the multiple reflections drew attention since early days. They are frequently too prevalent to overshadow the deep reflections, and the incorrect interpretation about them leads to the existence of the false reflector. Then an attempt to eliminate them is made and on the other hand, in order to identify them as the multiple reflection phase, the time interval between them, the move-out anomaly, the phase reversal, etc. are discussed in detail (24, 25, 26, 27, 28, 29, 30, 31, 32, 33, 34). And it is to be noted that their energies remain sufficiently strong to be recordable at surface after numerous multiple reflections. In the case of the present

study, it is also recognized that especially in the higher multiples, their amplitudes are too large relative to that of the direct  $P$ -wave. As mentioned above, the main effects ruling their amplitudes are theoretically in the reflection at the outer free surface and the Mohorovičić discontinuity of the base reflecting surface. But in reference to this point, the effects of the sedimentary layer as the low velocity contrast of the upper boundary may be considered to be likely those of the weathering layer in the seismic prospecting. Or, as in the marine survey, some sort of wave guide mechanism involving multiple reflection may be possible, and reinforcement by the constructive interference will also be suggestionable (35, 36, 37, 38, 39).

It is, however, one reasonable explanation for the anomalously large amplitude that the multiple reflections considered in the present study may be derived from the initially  $S$ -wave which is converted from  $S$  to  $P$  at the outer free surface. The considerable retardation of the travel times as a whole, namely from 5 to 10 sec in the present case (cf. Figs. 2 and 3) will then be also explained.

#### 4. Summary

Generally speaking, in shallow earthquake's record, the part between the initial  $P$ -motion and the principal  $S$ -motion is much more complicated than in deep earthquake's record. Considering the path along which the seismic waves are transmitted, the cause of this complexity is the complex structure of the earth's crust.

In the present study, two shallow earthquakes are selected and their seismograms recorded at 32 stations in the distance range from about 100 km to 600 km are studied concurrently. The various phases in the part from the initial  $P$ -motion to the principal  $S$ -motion are traced not only in their travel time but also in amplitude and period. Then the repetitive features of pulses in about equal time interval are interpreted as the multiple reflections between the outer free surface and the Mohorovičić discontinuity.

It was found especially that the difference of the time interval in the two cases of the selected earthquake, corresponds to the local difference of the thickness of the crust through which they are transmitted. Moreover, the identification of these multiple reflections is verified by the amplitude- and period-distance relations. On the amplitude and period variation with distance, more precise measurements are desirable which will offer the more interesting informations about the earth's crust.

#### Acknowledgments

The writer wishes to express his hearty thanks to Prof. E. Nishimura for his kind guidance and encouragement throughout the present study. The writer is also indebted to the directors and members of the Japan Meteorological Agency concerned in this study for their generous permission for copying seismograms recorded at their

observatories. The cost of the present study was partly defrayed by a grant-in-aid for scientific research of the Ministry of Education.

## REFERENCES

1. H. JEFFREYS, *The Earth*, (3rd ed., Cambridge University Press, 1952).
2. K. E. BULLEN, *An Introduction to the Theory of Seismology*, (2nd ed., Cambridge University Press, 1953).
3. K. SAGISAKA and M. TAKEHANA, On the surface reflections in near earthquake, *Kenshin-Ziho*, 8 (1935), 53-74 (in Japanese).
4. V. CONRAD, Das Schwadorfer Beben vom 8. Oktober 1927, *Gerl. Beitr. z. Geophys.*, 20 (1928), 240-277.
5. B. GUTENBERG, Travel time curves at small distances, and wave velocities in Southern California, *ibid.*, 35 (1932), 16-50.
6. T. UTSU, Some remarkable phases on seismograms of near earthquakes (Part I), *Kenshin-Ziho*, 20 (1956), 13-16 (in Japanese).
7. T. MATUZAWA und T. FUKUTOMI, Zwei merkwürdige Wellengruppen bei einigen Erdbeben in Kantô und die dritte Mitteilung über den vorlaufenden Teil der Erdbebenbewegungen, *Bull. Earthq. Res. Inst.*, 10 (1932), 499-516.
8. P. L. WILLMORE, A. L. HALES and P. G. GANE, A seismic investigation of crustal structure in the Western Transvaal, *Bull. Seism. Soc. America*, 42 (1952), 53-80.
9. E. R. LAPWOOD, Study of a series of Japanese earthquakes, *Mon. Not. Roy. Astr. Soc., Geophys. Suppl.*, 7 (1955), 135-146.
10. The Seismological Bulletin for March, 1952, (The Central Meteorological Observatory, Tokyo, Japan, 1952).
11. The Seismological Bulletin for July, 1955, (The Central Meteorological Observatory, Tokyo, Japan, 1955).
12. Y. KISHIMOTO, Seismometric investigation of the earth's interior, Part I. On the structure of the earth's upper layer, *Mem. Coll. Sci., Kyoto Univ.*, A, 27 (1954), 125-143.
13. ———, Ditto, Part II. On the structure of the earth's crust, *ibid.*, A, 27 (1955), 243-288.
14. A. KAMITSUKI, On the seismic waves reflected at the Mohorovičić discontinuity (I), *ibid.*, A, 28 (1956), 143-159.
15. H. JEFFREYS, Reflexion and refraction of elastic waves, *Mon. Not. Roy. Astr. Soc., Geophys. Suppl.*, 1 (1926), 321-334.
16. B. GUTENBERG, Energy ratio of reflected and refracted seismic waves, *Bull. Seism. Soc. America*, 34 (1944), 85-102.
17. ———, Reflected and minor phases in records of near-by earthquakes in Southern California, *ibid.*, 34 (1944), 137-160.
18. H. KAWASUMI and T. SUZUKI, Reflection and refraction of seismic waves at plane interface of the earth's crust, *Zisin*, 4 (1932), 277-307 (in Japanese).
19. M. MUSKAT and M. W. MERES, Reflection and transmission coefficients for plane waves in elastic media, *Geophysics* 5 (1940), 115-148.
20. L. B. SLICHTER and V. G. GABRIEL, Studies in reflected seismic waves, *Gerl. Beitr. z. Geophys.*, 38 (1933), 228-256.
21. T. MATUZAWA, An example of surface reflection of elastic plane waves, *Zisin*, 4 (1932), 7-12 (in Japanese).
22. L. KNOPOFF, R. W. FREDRICKS, A. F. GANGI and L. D. PORTER, Surface amplitudes of reflected body waves, *Geophysics*, 22 (1957), 842-847.
23. B. GUTENBERG, Revised travel times in Southern California, *Bull. Seism. Soc. America*, 41 (1951), 143-163.

24. L. DON LEET, Some Phases on explosion records in a 3-layered region, *Gerl. Beitr. z. Geophys.*, **42** (1934), 246-251.
25. ———, Trial travel times for Northern America, *Bull. Seism. Soc. America*, **31** (1941), 325-334.
26. T. P. ELLSWORTH, Multiple reflections, *Geophysics*, **13** (1948), 1-18.
27. CURTIS H. JOHNSON, Remarks regarding multiple reflections, *ibid.*, **13** (1948), 19-26.
28. JOHN SLOAT, Identification of echo reflections, *ibid.*, **13** (1948), 27-35.
29. B. GUTENBERG and C. Y. FU, Remarks on multiple reflections, *ibid.*, **13** (1948), 45-48.
30. RAUL F. HANSEN, Multiple reflections of seismic energy, *ibid.*, **13** (1948), 58-85.
31. ARNE JUNGER, Deep basement reflections in Big Horn County, Montana, *ibid.*, **16** (1951), 499-505.
32. THOS. C. POULTER and LEONARD V. LOMBARDI, Multiple reflections on the Edwards Plateau, *ibid.*, **17** (1952), 107-115.
33. M. TATSUGAMI, On the multiple reflections in Ariake District, *Butsuri-Tanko*, **8** (1955), 1-8 (in Japanese).
34. GLEN H. SWENUMSON, Geophysical case history of the Anderson Ranch Field, Lea County, New Mexico, *Geophysics*, **22** (1957), 870-886.
35. K. E. BURG, M. EWING, F. PRESS and E. T. STULKEN, A seismic wave guide phenomenon, *ibid.*, **16** (1951), 594-612.
36. GEORGE P. SARRAFIAN, A marine seismic model, *ibid.*, **21** (1956), 320-336.
37. M. EWING and F. PRESS, *Surface Waves and Guided Waves, Handbuch der Physik* (Springer-Verlag, 1957) Bd. **47**, 119-139.
38. B. GUTENBERG, Channel waves in the earth's crust, *Geophysics*, **20** (1955), 283-294.
39. F. PRESS and B. GUTENBERG, Channel *P* waves *IIg* in the earth's crust, *Trans. Amer. Geophys. Union*, **37** (1956), 754-756.

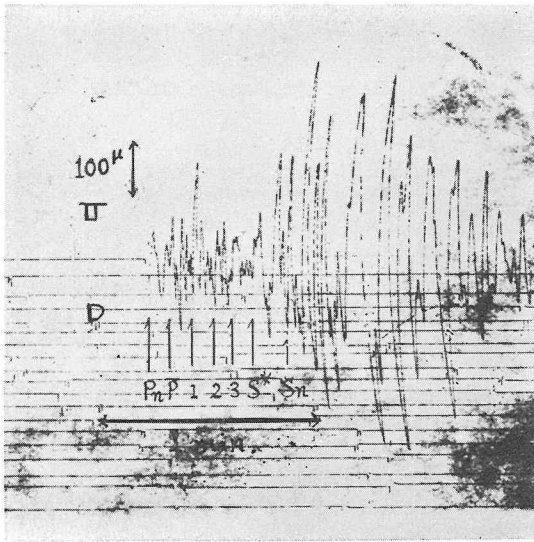


Fig. 4. Vertical Wiechert-seismogram, the Daishoji-Oki Earthquake, Sumoto ( $\Delta=265$  km). (By the courtesy of the Sumoto Meteorological Observatory)

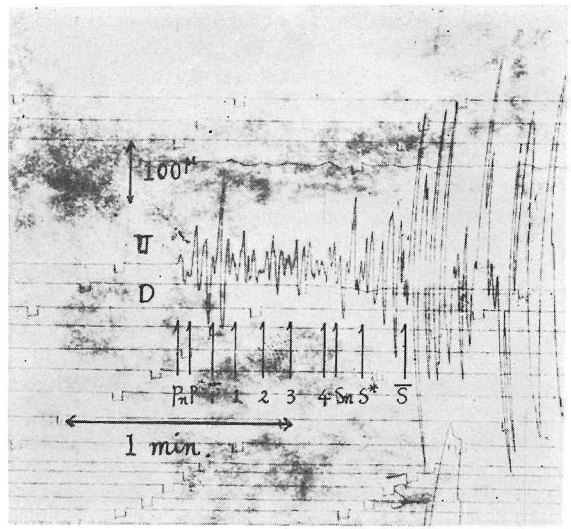


Fig. 5. Vertical Wiechert-seismogram, the Daishoji-Oki Earthquake, Hiroshima ( $\Delta=419$  km). (By the courtesy of the Hiroshima Meteorological Observatory)

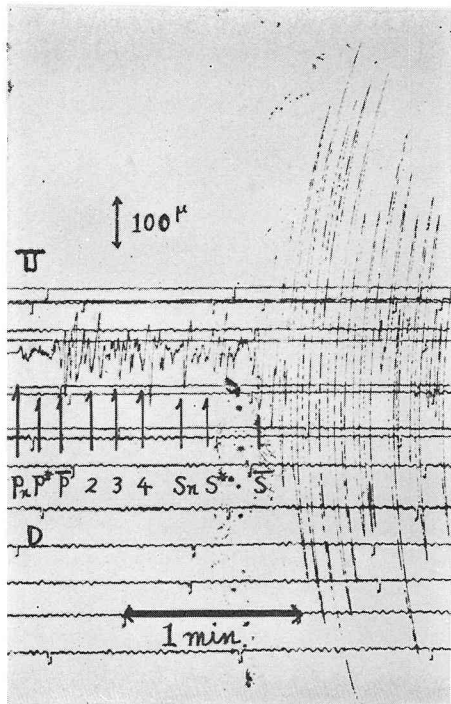


Fig. 6. Vertical Wiechert-seismogram, the Daishoji-Oki Earthquake, Oita ( $\Delta=552$  km). (By the courtesy of the Oita Meteorological Observatory)

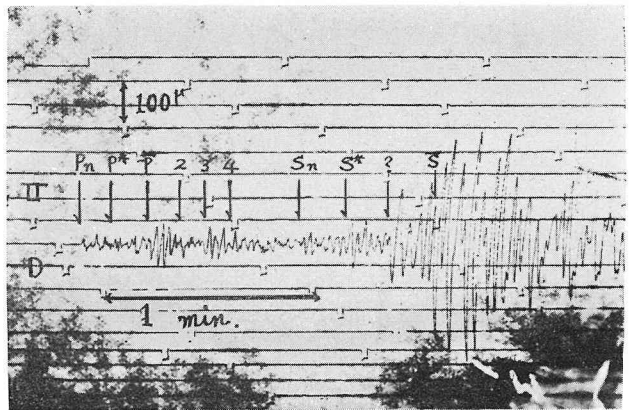


Fig. 7. Vertical Wiechert-seismogram, the Daishoji-Oki Earthquake, Kumamoto ( $\Delta=647$  km). (By the courtesy of the Kumamoto Meteorological Observatory)



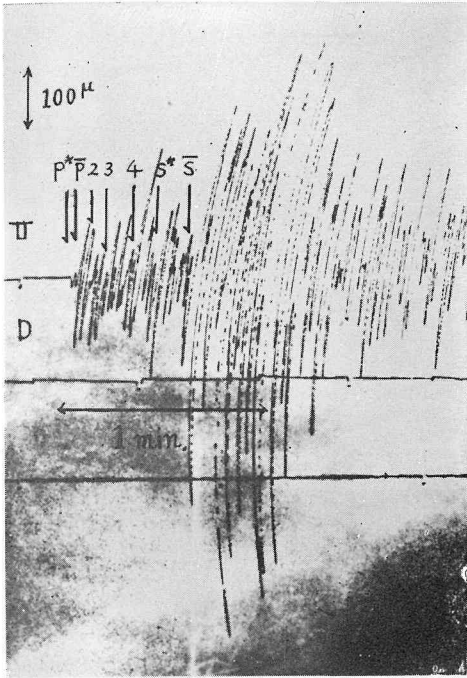


Fig. 8. Vertical Wiechert-seismogram, the Tokushima Earthquake, Oita ( $\Delta=256$  km). (By the courtesy of the Oita Meteorological Observatory)

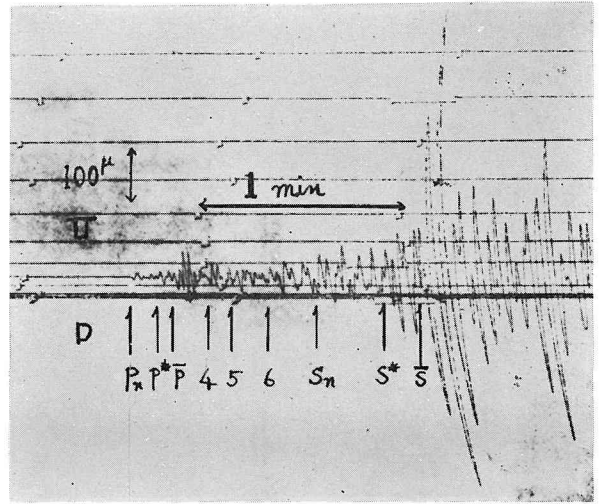


Fig. 10. Vertical Wiechert-seismogram, the Tokushima Earthquake, Kumagaya ( $\Delta=536$  km). (By the courtesy of the Kumagaya Meteorological Observatory)

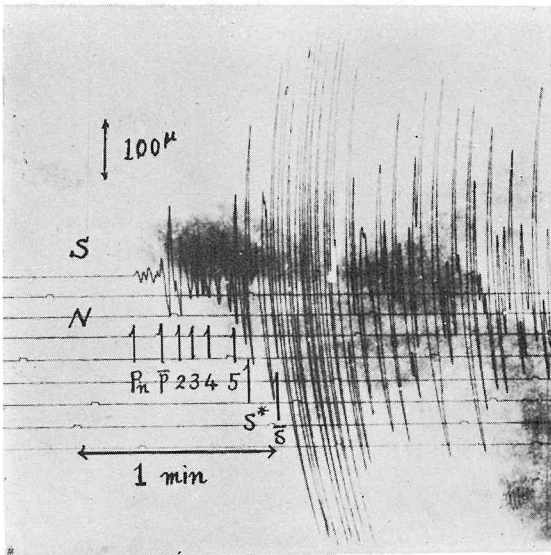


Fig. 9 a. Horizontal Wiechert-seismogram, the Tokushima Earthquake, Gifu ( $\Delta=291$  km). (By the courtesy of the Gifu Meteorological Observatory)

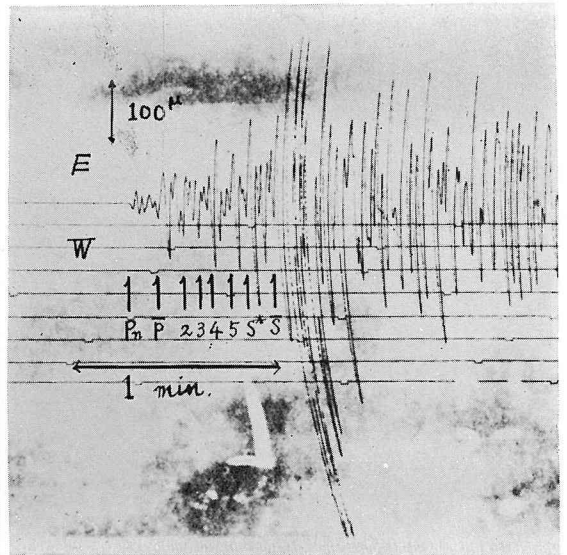


Fig. 9 b. Horizontal Wiechert-seismogram, the Tokushima Earthquake, Gifu ( $\Delta=291$  km). (By the courtesy of the Gifu Meteorological Observatory)

